**Supplementary information of https://doi.org/10.1631/jzus.B2500424**

## Section S1: performance evaluation metrics

To evaluate the performance of different methods in inferring gene regulatory networks (GRNs), we choose area under the receiver operating characteristic curve (AUROC) and area under the precision-recall curve (AUPRC) as metrics. AUROC represents the area under the curve of true positive rate against false positive rate, while AUPRC denotes the area under the curve of precision against recall. Higher AUROC and AUPRC scores indicate better performance of the corresponding methods and more accurate and reliable inferred GRNs.

$$\mathrm{FPR}=\frac{\mathrm{FP}}{\mathrm{FP+TN}}, \tag{S1}$$

$$\mathrm{TPR}=\frac{\mathrm{FP}}{\mathrm{TP+FN}}, \tag{S2}$$

$$\mathrm{Precision}=\frac{\mathrm{TP}}{\mathrm{TP+FP}}, \tag{S3}$$

$$\mathrm{Recall}=\frac{\mathrm{TP}}{\mathrm{TP+FN}}, \tag{S4}$$

$$\mathrm{AUROC}=\int_0^1 \mathrm{TPR}(\mathrm{FPR})\cdot \mathrm{dFPR}, \tag{S5}$$

$$\mathrm{AUPRC}=\int_0^1 \mathrm{Precision}(\mathrm{Recall})\cdot \mathrm{dRecall}, \tag{S6}$$

where TP denotes the number of true regulatory edges predicted to be positive, FN denotes the number of true regulatory edges predicted to be negative, FP denotes the number of false regulatory edges predicted to be positive, and TN denotes the number of false regulatory edges predicted to be negative.

## Section S2: summary of supplementary tables

**Table S1 Performance comparison between scGRAIL and its six variants under the AUROC metric on a TF500+ scale Specific class real network dataset**

| Variant/ dataset | TF500+ | | | | | | |
|---|---|---|---|---|---|---|---|
| | hESC | hHEP | mDC | mESC | mHSC-E | mHSC-GM | mHSC-L |
| w/o N | 0.866 | 0.889 | 0.712 | 0.908 | 0.906 | 0.909 | 0.820 |
| w/o S | 0.864 | 0.868 | 0.707 | 0.902 | 0.906 | 0.899 | 0.857 |
| w/ M | 0.855 | 0.895 | 0.717 | 0.892 | 0.918 | 0.924 | 0.864 |
| w/ G | 0.867 | 0.897 | 0.705 | 0.902 | 0.916 | 0.921 | 0.863 |
| w/ A | 0.870 | 0.898 | 0.713 | 0.902 | 0.917 | 0.926 | 0.869 |
| w/ V | 0.859 | 0.891 | 0.704 | 0.917 | 0.915 | 0.924 | 0.864 |
| scGRAIL | 0.876 | 0.902 | 0.722 | 0.919 | 0.925 | 0.929 | 0.872 |

hESC: human embryonic stem cell; hHEP: human hepatocyte; mDC: mouse dendritic cell; mESC: mouse embryonic stem cell; mHSC-E: mouse hematopoietic stem cell-erythroid; mHSC-GM: mouse hematopoietic stem cell-granulocyte/monocyte; mHSC-L: mouse hematopoietic stem cell-lymphoid.

**Table S2 AUROC of scGRAIL on Non-Specific and STRING real networks using TF500+ and TF1000+ gene scale datasets, under varying batch_size and hidden_dim configurations**

| Dataset/AUROC | batch_size | | | | hidden_dim | | | |
|---|---|---|---|---|---|---|---|---|
| | 512 | 256 | 128 | 64 | [512,256] | [256,128] | [128,64] | [64,32] |
| Non-Specific 500+ | 0.738 | 0.770 | 0.742 | 0.746 | 0.727 | 0.736 | 0.770 | 0.737 |
| Non-Specific 1000+ | 0.730 | 0.758 | 0.730 | 0.758 | 0.732 | 0.741 | 0.758 | 0.721 |
| STRING 500+ | 0.862 | 0.880 | 0.717 | 0.872 | 0.866 | 0.873 | 0.880 | 0.871 |
| STRING 1000+ | 0.885 | 0.893 | 0.838 | 0.881 | 0.868 | 0.885 | 0.893 | 0.885 |

STRING: search tool for the retrieval of interacting genes/proteins; AUROC: area under the receiver operating characteristic curve.

**Table S3 Statistical results of the average running time of our scGRAIL versus six existing methods on four classes of real networks and different gene-size datasets**

| Item | Average running time (s) | | | |
|---|---|---|---|---|
| | Lofgof | Non-Specific | Specific | STRING |
| scGRAIL | 7.79 | 3.88 | 28.67 | 5.84 |
| scMGATGRN | 75.76 | 76.31 | 367.57 | 100.04 |
| GENELink | 44.70 | 27.42 | 204.62 | 34.12 |
| GCLink | 29.50 | 19.61 | 140.28 | 24.52 |
| DeepRIG | 104.12 | 89.24 | 107.30 | 122.92 |
| DeepSEM | 107.27 | 120.53 | 116.12 | 118.75 |
| DGRNS | 332.07 | 257.63 | 1515.18 | 381.21 |

STRING: search tool for the retrieval of interacting genes/proteins.

**Table S4 Performance comparison (AUROC and AUPRC) of scGRAIL on the Specific network datasets of TF500+ and TF1000+ gene scales under unimputed and DeepImpute imputed statuses**

| Item | TF500+ | | TF1000+ | |
|---|---|---|---|---|
| | Unimputed | Imputed | Unimputed | Imputed |
| Dataset/AUROC | | | | |
| hESC | 0.732 | 0.877 | 0.877 | 0.880 |
| hHEP | 0.731 | 0.902 | 0.903 | 0.904 |
| mDC | 0.816 | 0.816 | 0.755 | 0.770 |
| mESC | 0.806 | 0.920 | 0.927 | 0.927 |
| mHSC-E | 0.779 | 0.928 | 0.937 | 0.938 |
| mHSC-GM | 0.779 | 0.928 | 0.936 | 0.939 |
| mHSC-L | 0.748 | 0.869 | 0.891 | 0.895 |
| Dataset/AUPRC | | | | |
| hESC | 0.877 | 0.880 | 0.615 | 0.620 |
| hHEP | 0.903 | 0.904 | 0.847 | 0.848 |
| mDC | 0.755 | 0.770 | 0.144 | 0.158 |
| mESC | 0.927 | 0.927 | 0.855 | 0.860 |
| mHSC-E | 0.937 | 0.938 | 0.952 | 0.952 |
| mHSC-GM | 0.936 | 0.939 | 0.946 | 0.950 |
| mHSC-L | 0.891 | 0.895 | 0.884 | 0.891 |

hESC: human embryonic stem cell; hHEP: human hepatocyte; mDC: mouse dendritic cell; mESC: mouse embryonic stem cell; mHSC-E: mouse hematopoietic stem cell-erythroid; mHSC-GM: mouse hematopoietic stem cell-granulocyte/monocyte; mHSC-L: mouse hematopoietic stem cell-lymphoid; AUROC: area under the receiver operating characteristic curve; AUPRC: area under the precision-recall curve.

**Table S5 Performance landscape of scGRAIL versus the other four models under different proportions of noise interference on three mouse datasets (mHSC-E, mHSC-GM, and mHSC-L) at the TF500+ gene scale in the Specific-like real network**

| Dataset | Model | AUROC | | | | |
|---|---|---|---|---|---|---|
| | | 0% | 10% | 20% | 30% | 40% |
| mHSC-E | scGRAIL | 0.925 | 0.919 | 0.912 | 0.909 | 0.903 |
| | GENELink | 0.884 | 0.804 | 0.734 | 0.502 | 0.754 |
| | GCLink | 0.895 | 0.886 | 0.883 | 0.886 | 0.885 |
| | GNNLink | 0.880 | 0.796 | 0.794 | 0.829 | 0.823 |
| | DeepRIG | 0.742 | 0.729 | 0.699 | 0.667 | 0.665 |
| mHSC-GM | scGRAIL | 0.928 | 0.923 | 0.915 | 0.905 | 0.898 |
| | GENELink | 0.900 | 0.818 | 0.841 | 0.791 | 0.742 |
| | GCLink | 0.905 | 0.908 | 0.903 | 0.896 | 0.894 |
| | GNNLink | 0.890 | 0.876 | 0.872 | 0.869 | 0.876 |
| | DeepRIG | 0.636 | 0.700 | 0.643 | 0.672 | 0.666 |
| mHSC-L | scGRAIL | 0.872 | 0.859 | 0.856 | 0.855 | 0.850 |
| | GENELink | 0.841 | 0.817 | 0.775 | 0.784 | 0.773 |
| | GCLink | 0.828 | 0.842 | 0.838 | 0.838 | 0.837 |
| | GNNLink | 0.850 | 0.833 | 0.831 | 0.839 | 0.839 |
| | DeepRIG | 0.656 | 0.694 | 0.567 | 0.518 | 0.504 |

mHSC-E: mouse hematopoietic stem cell-erythroid; mHSC-GM: mouse hematopoietic stem cell-granulocyte/monocyte; mHSC-L: mouse hematopoietic stem cell-lymphoid.

## Section S3: supplementary data for case studies

As shown in Fig. S1, among the top 200 high-confidence prediction edges for the TF1000+ gene scale, 183 are known regulatory relationships in the standard network, 1 exists in the STRING network, and 16 are prediction edges that have not yet been covered by existing databases. The regulatory role of these key TFs has been confirmed by several literatures and databases, which further supports the biological plausibility of the model predictions.

In addition, we analyzed the top 20 TF–target gene regulatory pairs with the highest prediction scores in the hESC dataset, as shown in Table S6, and all of these prediction edges have been validated in standard networks.

In summary, scGRAIL is not only capable of accurately restoring known gene regulatory relationships, but also has the ability to mine potential regulatory mechanisms, which provides a basis for researchers to screen subsequent experimental targets and lays the foundation for improving biological regulatory data.

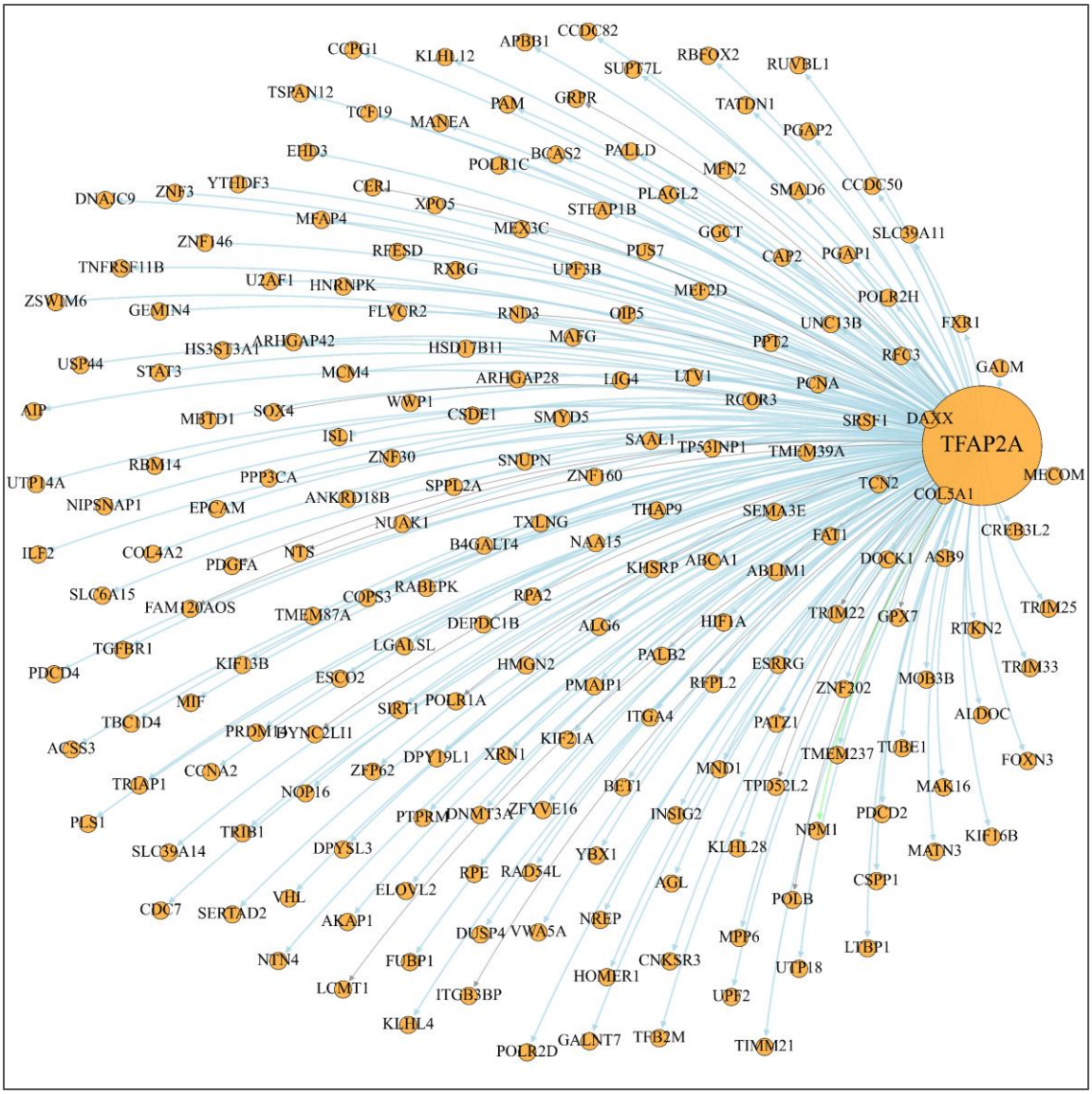



**Fig. S1 Top 200 TF–target gene regulatory pairs with the highest model prediction scores on the hESC dataset (TF1000+) of the Specific-like network. TF: transcription factor; hESC: human embryonic stem cells.**

**Table S6 Top 20 high-confidence TF–target gene pairs inferred by scGRAIL on the hESC datasets (TF500+ and TF1000+) of the Specific-like network (Diacou et al., 2022; Wang et al., 2024)**

| No. | Specific network | | | |
|---|---|---|---|---|
| | hESC-TF500+ | | hESC-TF1000+ | |
| | TF | Target | TF | Target |
| 1 | TFAP2A | NUP54 | TFAP2A | SLC39A11 |
| 2 | TFAP2A | SALL2 | TFAP2A | CDC7 |
| 3 | TFAP2A | PHB2 | TFAP2A | DNAJC9 |
| 4 | TFAP2A | ZNF202 | TFAP2A | RUVBL1 |
| 5 | TFAP2A | EEF1A1 | TFAP2A | TCF19 |
| 6 | TFAP2A | ANKRD28 | TFAP2A | NAA15 |
| 7 | TFAP2A | DNMT3A | TFAP2A | SLC39A14 |
| 8 | TFAP2A | RGS5 | TFAP2A | TGFBR1 |
| 9 | TFAP2A | FUBP1 | TFAP2A | DNMT3A |
| 10 | TFAP2A | CDCA2 | TFAP2A | INSIG2 |
| 11 | TFAP2A | HNRNPD | TFAP2A | ZFP62 |
| 12 | TFAP2A | ETV1 | TFAP2A | KIF21A |
| 13 | TFAP2A | CSDE1 | TFAP2A | POLR1C |
| 14 | TFAP2A | TCF4 | TFAP2A | ILF2 |
| 15 | TFAP2A | SNRPB | TFAP2A | TFB2M |
| 16 | TFAP2A | SIRT1 | TFAP2A | XPO5 |
| 17 | TFAP2A | BCAR3 | TFAP2A | RFC3 |
| 18 | TFAP2A | FAM117B | TFAP2A | FUBP1 |
| 19 | TFAP2A | SFPQ | TFAP2A | MAK16 |
| 20 | TFAP2A | BRWD1 | TFAP2A | PDCD4 |

hESC: human embryonic stem cell; TF: transcription factor; TFAP2A: transcription factor AP-2 alpha; NUP54: nucleoporin 54; SALL2: spalt like transcription factor 2; PHB2: prohibitin 2; ZNF202: zinc finger protein 202; EEF1A1: eukaryotic translation elongation factor 1 alpha 1; ANKRD28: ankyrin repeat domain 28; DNMT3A: DNA methyltransferase 3 alpha; RGS5: regulator of G protein signaling 5; FUBP1: far upstream element binding protein 1; CDCA2: cell division cycle associated 2; HNRNPD: heterogeneous nuclear ribonucleoprotein D; ETV1: ETS variant transcription factor 1; CSDE1: cold shock domain containing E1; TCF4: transcription factor 4; SNRPB: small nuclear ribonucleoprotein polypeptides B and B1; SIRT1: sirtuin 1; BCAR3: breast cancer anti-estrogen resistance 3; FAM117B: family with sequence similarity 117 member B; SFPQ: splicing factor proline and glutamine rich; BRWD1: bromodomain and WD repeat domain containing 1; SLC39A11: solute carrier family 39 member 11; CDC7: cell division cycle 7; DNAJC9: DnaJ heat shock protein family (Hsp40) member C9; RUVBL1: RuvB like AAA ATPase 1; TCF19: transcription factor 19; NAA15: N-alpha-acetyltransferase 15; SLC39A14: solute carrier family 39 member 14; TGFBR1: transforming growth factor beta receptor 1; INSIG2: insulin induced gene 2; ZFP62:zinc finger protein 62; KIF21A: kinesin family member 21A; POLR1C: RNA polymerase I subunit C; ILF2:interleukin enhancer binding factor 2; TFB2M: transcription factor B2, mitochondrial; XPO5: exportin 5; RFC3: replication factor C subunit 3; MAK16: MAK16 homolog; PDCD4: programmed cell death 4.

## References


Diacou R, Nandigrami P, Fiser A, et al., 2022. Cell fate decisions, transcription factors and signaling during early retinal development. *Prog Retin Eye Res*, 91:101093. https://doi.org/10.1016/j.preteyeres.2022.101093

Wang DG, Gao J, Wang J, et al., 2024. TFAP2A drives non-small cell lung cancer (NSCLC) progression and resistance to targeted therapy by facilitating the ESR2-mediated MAPK pathway. *Cell Death Discov*, 10(1):491. https://doi.org/10.1038/s41420-024-02251-5